Inorganic Chemistry

Article

pubs.acs.org/IC

Four Metalloporphyrinic Frameworks as Heterogeneous Catalysts for Selective Oxidation and Aldol Reaction

Chao Zou,[†] Tianfu Zhang,[‡] Ming-Hua Xie,[†] Lijun Yan,[‡] Guo-Qiang Kong,[†] Xiu-Li Yang,[†] An Ma,*[,‡] and Chuan-De Wu*[,†]

[†]Department of Chemistry, Zhejiang University, Hangzhou 310027, China

[‡]Petrochemical Research Institute, Petrochina Company Limited, Beijing 100083, China

Supporting Information

ABSTRACT: Four porous metalloporphyrinic framework materials, $[(CH_3)_2NH_2][Zn_2(HCOO)_2(Mn^{III}–TCPP)]\cdot 5DMF\cdot 2H_2O$ (**1**; H_6TCPP = tetrakis(4-carboxyphenyl)porphyrin), $[(CH_3)_2NH_2]$-$[Cd_2(HCOO)_2(Mn^{III}–TCPP)]\cdot 5DMF\cdot 3H_2O$ (**2**), $[Zn_2(HCOO)$-$(Fe^{III}(H_2O)–TCPP)]\cdot 3DMF\cdot H_2O$ (**3**), and $[Cd_3(H_2O)_6(\mu_2\text{-}O)(Fe^{III}–HTCPP)_2]\cdot 5DMF$ (**4**) were synthesized by heating a mixture of $M^{III}Cl–H_4TCPP$ (M = Mn and Fe) and M′ (M′ = Zn or Cd) nitrate in a mixed solvent of DMF and acetic acid. Compounds **1**–**3** are built up from $M'_2(COO)_4$ paddle-wheel subunits bridged by M^{III}–TCPP and formate ligands to form their 3D connections. The formate pillar heterogeneously connects with M and M′ cations in **1** and **2** and homogeneously joins M′ cations in **3**. The μ_2-O bridged Fe^{III}–HTCPP dimer performs as a decadentate ligand to link 10 cadmium cations for the formation of an interesting 3D coordination network of **4**. The four porphyrinic frameworks present interesting catalytic properties in the selective epoxidation of olefins, oxidation of cyclohexane, and intermolecular aldol reaction of aldehydes and ketones.

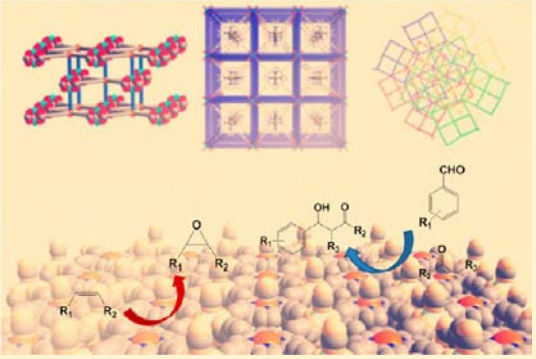

INTRODUCTION

Metal–organic frameworks (MOFs) are a remarkable class of porous materials with intriguing structural patterns and fascinating properties.[1] Compared with traditional inorganic zeolites, the pore dimensions and properties of MOFs are predictable and controllable with designed building synthons.[2] The variable modular constituents lead to a variety of MOFs with great potentials for a number of applications in the fields of luminescence, gas storage, sensing, and magnetics.[3−6] It is an interesting topic to develop useful platforms for heterogeneous catalysis by uniformly dispersing homogeneous catalysts on the channel walls of porous MOFs.[2] As an emerging class of porous materials, the advantage of crystalline MOF catalysts over conventional inorganic catalysts lies in the clearly demonstrated framework–functionality relationship. Among the reported heterogeneous catalysts, the porosity of MOFs and the accessibility of active metal sites are demonstrated significantly important for chemical transformations.[7,8]

Because of their unique biological and chemical characters, metalloporphyrins represent a remarkable class of constituent elements in a variety of synthetic materials with a range of applications.[9] The remarkable catalytic ability of metalloporphyrins makes them be an ideal class of building synthons for crystal engineering of functional MOFs as a unique chemical platform for biomimetic catalysis with heme analogues in control over porous ambient.[10,11]

Attracted by the high biomimetic catalytic efficiency of metalloporphyrins, we have synthesized a series of functional porphyrinic MOFs.[11] To further understand the structure–property relationship, herein we report four 3D metalloporphyrinic MOFs $[(CH_3)_2NH_2][Zn_2(HCOO)_2(Mn^{III}–TCPP)]\cdot 5DMF\cdot 2H_2O$ (**1**), $[(CH_3)_2NH_2]$-$[Cd_2(HCOO)_2(Mn^{III}–TCPP)]\cdot 5DMF\cdot 3H_2O$ (**2**), $[Zn_2(HCOO)(Fe^{III}(H_2O)–TCPP)]\cdot 3DMF\cdot H_2O$ (**3**), and $[Cd_3(H_2O)_6(\mu_2\text{-}O)(Fe^{III}–HTCPP)_2]\cdot 5DMF$ (**4**) with interesting catalytic properties for selective oxidation of hydrocarbons and intermolecular aldol reaction of aldehydes and ketones.

EXPERIMENTAL SECTION

Materials and Methods. All of the chemicals were obtained from Sinopharm Chemical Reagent Limited Company and were used without further purification. Tetrakis(4-carboxyphenyl)porphyrin (H_6TCPP), $Mn^{III}Cl–H_4TCPP$, and $Fe^{III}Cl–H_4TCPP$ were synthesized according to the literature.[12] IR spectra were recorded from KBr pellets on a FTS-40 spectrophotometer. Thermogravimetric analyses (TGA) were carried out under nitrogen on a NETZSCH STA 409 PC/PG instrument at a heating rate of 10 °C/min. GC-MS was recorded on a SHIMADZU GCMS-QP2010. SEM images were recorded on a Philips XL30ESEM equipment. Elemental analyses were performed on a ThermoFinnigan Flash EA 1112 element analyzer. ^1H NMR spectra were recorded on a 500 MHz spectrometer in $CDCl_3$ solution and the chemical shifts were reported relative to internal standard TMS (0 ppm).

Received: September 6, 2012
Published: March 21, 2013

   dx.doi.org/10.1021/ic3019502 | Inorg. Chem. 2013, 52, 3620–3626

Synthesis of $[(CH_3)_2NH_2][Zn_2(HCOO)_2(Mn^{III}$–TCPP)]·5DMF·2H$_2$O (1). A mixture of MnCl–H_4TCPP (20 mg, 0.023 mmol) and $Zn(NO_3)_2·6H_2O$ (20 mg, 0.067 mmol) in a mixed solvent of DMF (10 mL) and acetic acid (1 mL) was sealed in a screw cap vial and heated at 80 °C for five days. Deep-brown crystals of **1** were filtered, washed with EtOH and ethyl ether, and dried in the air. Yield: 15 mg (51%). Compound **1** is slightly soluble in water but very stable in common organic solvents, such as DMF, THF, CH_2Cl_2, EtOH, and acetone, and so forth. Anal. Calcd for $C_{67}H_{73}N_{10}O_{19}Zn_2Mn$ (%): C, 53.36; H, 4.88; N, 9.29. Found (%): C, 53.34; H, 4.72; N, 9.16. IR (KBr pellet): ν/cm^{-1} = 3408 (m), 1701 (w), 1605 (s), 1547 (m), 1386 (s), 1348 (w), 1205 (w), 1177 (w), 1139 (w), 1100 (w), 1070 (w), 1011 (m), 870(w), 830 (w), 802 (w), 777 (w), 718 (w), 668 (w), 632 (w), 610 (w), 580 (w), 489 (w), 406 (w).

Synthesis of $[(CH_3)_2NH_2][Cd_2(HCOO)_2(Mn^{III}$–TCPP)]·5DMF·3H$_2$O (2). A mixture of MnCl–H_4TCPP (20 mg, 0.023 mmol) and $Cd(NO_3)_2·4H_2O$ (20 mg, 0.065 mmol) in a mixed solvent of DMF (10 mL) and acetic acid (1 mL) was sealed in a screw cap vial and heated at 80 °C for five days. Deep-brown crystals of **2** were filtered, washed with EtOH and ethyl ether, and dried in the air. Yield: 15 mg (40%). Compound **2** is slightly soluble in water but very stable in common organic solvents, such as DMF, THF, CH_2Cl_2, EtOH, and acetone, and so forth. Anal. Calcd for $C_{67}H_{75}N_{10}O_{20}Cd_2Mn$ (%): C, 49.67; H, 4.67; N, 8.65. Found (%): C, 49.79; H, 4.63; N, 8.69. IR (KBr pellet): ν/cm^{-1} = 3425 (m), 1654 (m), 1601 (m), 1585 (m), 1536 (m), 1390 (s), 1341 (w), 1278 (w), 1204 (w), 1177 (w), 1140 (w), 1101 (w), 1011 (m), 870 (w), 852 (w), 830 (w), 804 (w), 777 (w), 718 (w), 669 (w), 637 (w), 613 (w), 570 (w), 491 (w).

Synthesis of $[Zn_2(HCOO)(Fe^{III}(H_2O)$–TCPP)]·3DMF·H$_2$O (3). A mixture of FeCl–H_4TCPP (28 mg, 0.032 mmol) and $Zn(NO_3)_2·6H_2O$ (30 mg, 0.1 mmol) in a mixed solvent of DMF (6 mL) and acetic acid (0.5 mL) was sealed in a screw cap vial and heated at 80 °C for five days. Deep brown crystals of **3** were filtered, washed with EtOH and ethyl ether, and dried in the air. Yield: 28 mg (68%). Compound **3** is slightly soluble in water but very stable in common organic solvents, such as DMF, THF, CH_2Cl_2, EtOH, and acetone, and so forth. Anal. Calcd for $C_{58}H_{50}N_7O_{15}FeZn_2$ (%): C, 54.78; H, 3.96; N, 7.71. Found: C, 53.88; H, 4.12; N, 7.72. IR (KBr pellet): ν/cm^{-1} = 3423 (m), 1605 (s), 1544 (m), 1385 (m), 1330 (w), 1203 (w), 1178 (w), 1138 (w), 1101 (w), 1068 (w), 1000 (m), 871 (w), 840 (w), 801 (w), 777 (w), 720 (w), 668 (w), 638 (w), 587 (w), 488 (w).

Synthesis of $[Cd_3(H_2O)_6(\mu_2$-O)$(Fe^{III}$–HTCPP)$_2$]·5DMF (4). Deep-brown crystals of **4** were synthesized similar to the procedure of **3**, except $Cd(NO_3)_2·4H_2O$ (31 mg, 0.1 mmol) was used instead of $Zn(NO_3)_2·6H_2O$. Deep-brown crystals of **4** were filtered, washed with EtOH and ethyl ether, and dried in the air. Yield: 26 mg (32%). Compound **4** is slightly soluble in water but very stable in common organic solvents, such as DMF, THF, CH_2Cl_2, EtOH and acetone, etc. Anal. Calcd for $C_{111}H_{97}N_{13}O_{28}Fe_2Cd_3$ (%): C, 53.12; H, 3.90; N, 7.25. Found: C, 51.86; H, 3.87; N, 7.22. IR (KBr pellet): ν/cm^{-1} = 3448 (m), 1655 (w), 1584 (m), 1537 (m), 1386 (s), 1203 (w), 1178 (w), 1102 (w), 1070 (w), 999 (m), 873 (w), 852 (w), 798 (w), 779 (w), 719 (w), 668 (w), 575 (w), 487 (w).

Single-Crystal X-ray Data Collections and Structure Determinations. The determinations of the unit cells and data collections for the crystals of **1**, **2**, **3**, and **4** were performed on an Oxford Xcalibur Gemini Ultra diffractometer with an Atlas detector. The data of compounds **1**, **2**, and **4** were collected using graphite–monochromatic Mo–Kα radiation (λ = 0.71073 Å) at 293 K, whereas the data of compound **3** were collected using graphite–monochromatic enhanced ultra Cu radiation (λ = 1.54178 Å) at 293 K. The data sets were corrected by empirical absorption correction using spherical harmonics implemented in SCALE3 ABSPACK scaling algorithm.[13] The structures were solved by direct methods and refined by full-matrix least-squares methods with the *SHELX-97* program package.[14] The solvent molecules in compounds **1**–**4** are highly disordered which could not be located successfully from Fourier maps in the refinement cycles. The scattering from the highly disordered lattice guest molecules were removed using the SQUEEZE procedure implemented in the *PLATON* package.[15] The resulting new files were used to further refine the structures. Because of the poor quality of the crystal data for compound **4**, only part atoms were refined anisotropically. The compositions of the as-synthesized compounds **1**–**4** were figured out based on the elemental analyses, TGA, and single-crystal structures. The lattice molecules were added to account for the formulas in the cif files. H atoms on C atoms were generated geometrically. All nonsolvent atoms were located successfully from Fourier maps.

Powder X-ray Diffraction Analysis. Powder X-ray diffraction (PXRD) data were recorded on a RIGAKU D/MAX 2550/PC for Cu–Kα radiation (λ = 1.5406 Å) at 293 K. A freshly prepared crystalline sample was mounted on a piece of quartz glass with a round discal concave for PXRD experiment. To make a comparison, several very large crystals were selected by hand under a microscope. Every selected crystal was subjected to single-crystal X-ray diffraction analysis to determine the unit cell dimensions. The combined single crystals were crushed by a medicine spoon for subsequent PXRD experiment.

Typical Procedure for Substrate Adsorption Experiments. A sample of **1** was heated at 90 °C under vacuum for 12 h, which was immersed in methanol solvent for 6 h at room temperature. The solid was filtered and thoroughly washed with ethyl ether to remove the surface adsorbed molecules. The solid was digested by dilute aqueous hydrochloric acid and extracted with hexane solvent. The identity and quantity of the adsorbed solvent molecules were determined by analyzing aliquots of the bulk solution using GC-MS with an external standard of chlorobenzene.

Typical Procedure for Epoxidation of Olefins. A mixture of catalyst **1** (0.01 mmol), styrene (0.1 mmol), and PhIO (0.15 mmol) in CH_2Cl_2 (1.5 mL) was stirred at room temperature for 6 h. The reaction mixture was filtrated. The recovered solid was washed with CH_2Cl_2 for three times and dried, which was subsequently used in the successive run and PXRD experiment. The identity of the product was determined by analyzing aliquots of the bulk solution with GC-MS and compared with the authentic samples analyzed under the same conditions, whereas the conversion and selectivity were obtained by GC analysis with a flame-ionization detector (FID) using a capillary SE-54 column. Every catalytic reaction was conducted for three times, and the yield is the average result of three runs.

Typical Procedure for Epoxidation of Styrene by Catalyst 1 with Different Particle Sizes. The samples of solid **1** were respectively ground in CH_2Cl_2 at room temperature for 1, 3, 6, and 9 h, whereas the particle sizes of the resulted solid samples were monitored by SEM images. The pretreated solid catalyst **1** (0.01 mmol) was added into a mixture of styrene (0.1 mmol) and PhIO (0.15 mmol) in CH_2Cl_2 (1.5 mL). After the mixture was reacted at room temperature for 12 h without stirring, the solid was filtered. The filtrate was subjected to GC-MS analysis with an FID using a capillary SE-54 column. Every catalytic reaction was conducted for three times, and the yield is the average result of three runs.

Study of the Traces of Styrene Oxide Yields versus Reaction Time Catalyzed by 1. Styrene (0.1 mmol), PhIO (0.15 mmol), and catalyst **1** (0.01 mmol) in CH_2Cl_2 (1.5 mL) were reacted at room temperature under or without stirring. The aliquots were regularly taken out for GC analysis to determine the yield of styrene oxide.

Typical Procedure for Oxidation of cyclohexane. A mixture of catalyst (0.01 mmol), cyclohexane (0.1 mmol), and PhIO (0.15 mmol) in CH_2Cl_2 (1.5 mL) was sealed in a small Teflon lined screw cap vial and stirred at room temperature for 6 h. The identity of the products was determined by analyzing aliquots of the bulk solution with GC-MS, and compared with the authentic samples analyzed under the same conditions, whereas the conversion and selectivity were obtained by GC analysis with an FID using a capillary SE-54 column. The results are the average results of three runs.

Typical Procedure for Aldol Reaction. A mixture of catalyst (0.005 mmol) and aldehyde (0.05 mmol) in ketone (1 mL) was stirred at 55 °C for 72 h. The mixture was diluted with 2 mL ethyl acetate and filtered. The recovered solid was washed with EtOH and ethyl ether and dried, which was subsequently used in the successive run. The

dx.doi.org/10.1021/ic3019502 | *Inorg. Chem.* 2013, 52, 3620–3626

filtrate was evaporated under reduced pressure at room temperature. The crude product was passed through a column of silica gel using petroleum ether and ethyl acetate (V/V = 10:1) as eluent followed by vacuum evaporation at room temperature. The identity of the product was determined by ^{1}H NMR spectroscopy, whereas the yield and diastereomeric ratio (d.r.) were obtained by HPLC analysis using an Ultimate XB-C18 column (5 μm, 4.6 × 250 mm^2). The yield and selectivity are the average results of three runs.

RESULTS AND DISCUSSION

The four metalloporphyrinic MOFs were synthesized by heating a mixture of M^{III}Cl−H$_4$TCPP (M = Mn and Fe) and

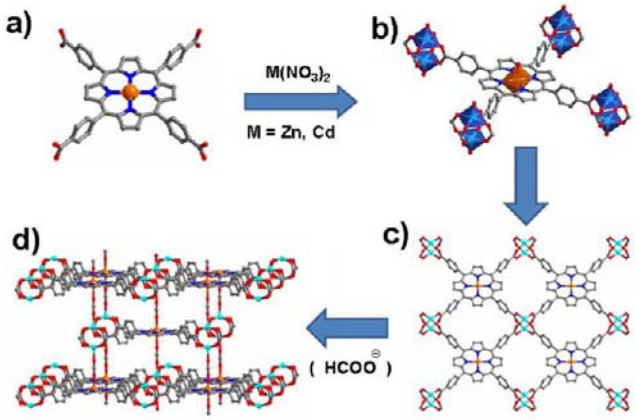

Figure 1. (a) Deprotonated Mn−TCPP ligand, (b) view of the coordination mode of Mn−TCPP and the coordination environments of M′ and Mn atoms, (c) lamellar network of Mn−TCPP linking up M′$_2$(COO)$_4$ paddle-wheel SBUs in **1**, (d) perspective view of the 3D porphyrinic framework. Color codes: M′, cyan or light-blue square-pyramids; Mn, orange; O, red; N, blue; C, gray.

M′ nitrate (M′ = Zn and Cd) in a mixed solvent of DMF and acetic acid. The disordered solvent molecules were counted according to elemental analysis, TGA, and single-crystal structures.

Single-crystal X-ray diffraction analysis revealed that compounds **1** and **2** are isomorphous, which crystallize in the tetragonal $I4/mmm$ space group.[16] The 3D structure is made up of a Mn(III)−TCPP metalloligand connected with four binuclear M′$_2$(COO)$_4$ (M′ = Zn or Cd) paddle-wheel secondary building units (SBUs) and a formate pillar (Figure 1).[17] The formate pillar heterogeneously connects with M′$_2$(COO)$_4$ SBU and porphyrin Mn^{III} cation in a non-interpenetrated AB stacking pattern of the 3D net.[18] There are two kinds of channels in the two porphyrinic frameworks with dimensions of ∼7.74 × 11.79 Å^2 along the a and b axes, and ∼11.79 × 11.79 Å^2 along the c axis, respectively. Unfortunately, the axial coordination sites of the manganese(III) cations are blocked by the formate struts. Hence, the active Mn^{III} sites are inaccessible to substrate molecules through the opening channels even though the vacant spaces are 61.4 and 64.0% for **1** and **2**, respectively.[19] The porphyrin Mn^{III} cations on the exterior solid surfaces are the only reachable catalytic sites for substrate molecules. TGA showed a weight loss of 26.1% occurred between 30 and 325 °C for **1** corresponding to the loss of DMF and H$_2$O molecules (expected 26.6%), whereas the loss of DMF and H$_2$O molecules for **2** occurred between 30 and 322 °C (expected 25.9%, observed 25.8%).

When Mn(III) cation was replaced by Fe(III) cation in the porphyrin ligand, the formate strut homogeneously links two

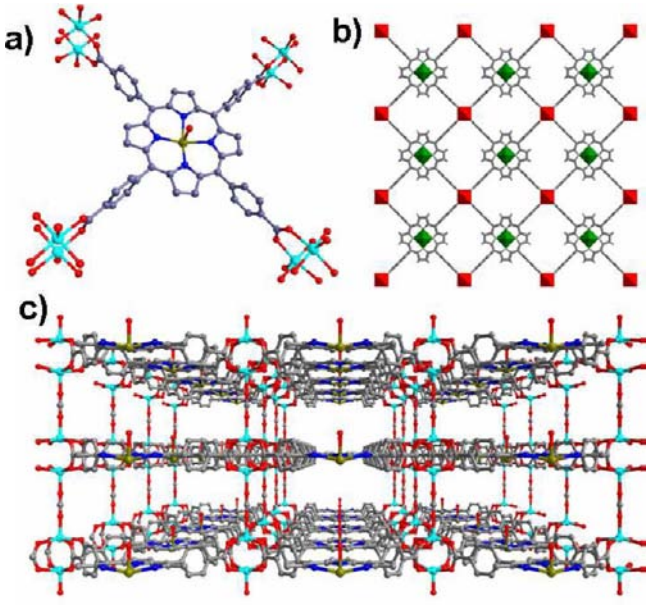

Figure 2. (a) View of the coordination mode of Fe^{III}−TCPP and the coordination environments of zinc and iron atoms, (b) lamellar network of Fe−TCPP linking up zinc paddle-wheel SBUs in **3** as viewed down the c axis, (c) perspective view of the 3D framework of **3** down the b axis showing the 3D opening channels and the well-dispersed Fe^{III} centers in the channel walls. Color codes: Zn, cyan or red square-pyramids; Fe, dark-yellow or green square-pyramids; O, red; N, blue; C, gray.

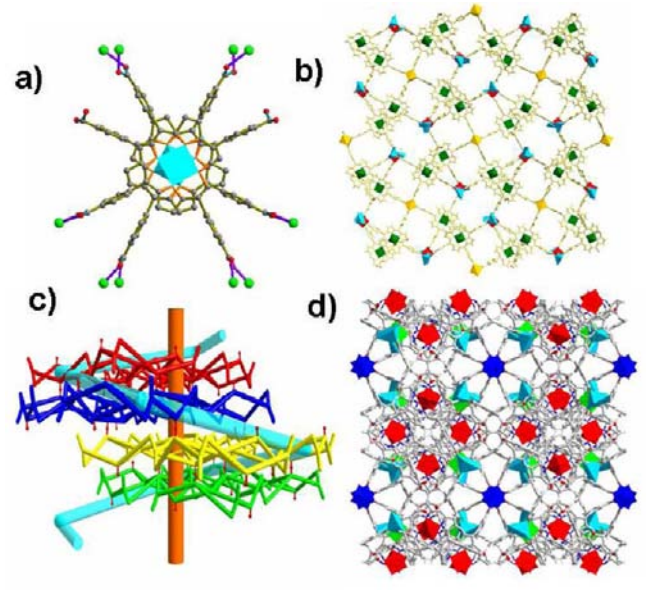

Figure 3. (a) View of the μ_2-O bridged Fe−HTCPP pair and the coordination mode in **4** (color codes: Cd, green; Fe, cyan square-pyramids; O, red; N, blue; C, gray), (b) lamellar network of Fe−HTCPP linking up cadmium polyhedra as viewed down the c axis (color codes: Cd, red, cyan or yellow polyhedra; Fe, green square-pyramids), (c) view of the relationship between different lamellae (represented as different colors) operated by the screw 4$_1$ axis along the a axis, (d) 3D framework of **4** as viewed down the c axis (color codes: Cd, blue, cyan or green polyhedra; Fe, red square-pyramids; O, red; N, blue; C, gray).

Zn$_2$(COO)$_4$ paddle-wheel SBUs to form a AA stacked 3D net of **3** that crystallizes in the tetragonal $P4/mmm$ space group

dx.doi.org/10.1021/ic3019502 | Inorg. Chem. 2013, 52, 3620−3626

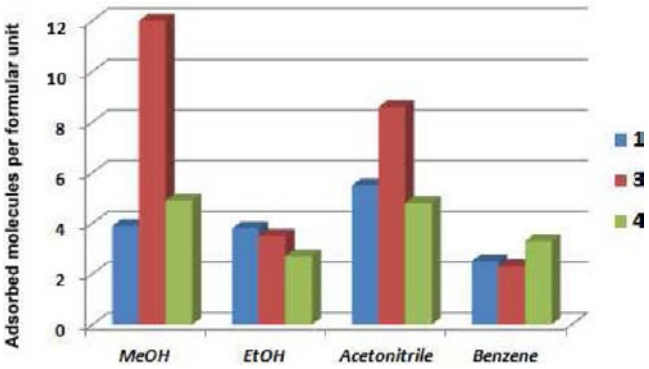

Figure 4. Illustration of the sorption ability of **1**, **3**, and **4** per formular unit as probed by GC-MS.

Table 1. Selective Epoxidation of Olefins[a]

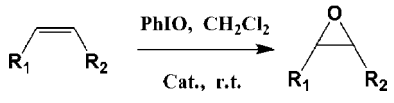

Entry	Substrate	Product	Yield%[b]	
			1	**L**[c]
1			>99	72.4[d]
2			>99[e]	72.4[d]
3			17.9[f]	72.4[d]
4			8.4[g]	72.4[d]
5			>99	>99
6			>99	29.3[d]
7			72.5	93.7[d]
8			>99	13.8[d]
9			64.9	25.3
10			42.5[d]	34.4[d]
11	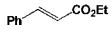	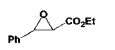	15.3	12.0
12	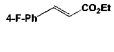	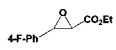	10.6	11.4
13	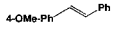	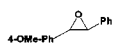	28.5	44.3
14	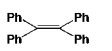	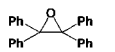	7.0	1.6

[a]Catalyst (0.01 mmol), substrate (0.1 mmol), and PhIO (0.15 mmol) in 5 mL CH_2Cl_2 were stirred at room temperature for 6 h. [b]On the basis of GC-MS analysis, an average value of three runs. [c]L = MnCl–Me_4TCPP. [d]Additional byproducts formed. [e–g]Catalyzed by **2**, **3**, and **4**, respectively.

Scheme 1. Oxidation of Cyclohexane Catalyzed by Solid 1

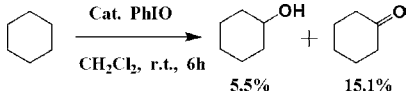

(Figure 2). Compound **3** contains two kinds of channels with dimensions of 8.86 × 16.67 Å^2 as viewed along the *a* and *b* axis, and 11.81 × 11.81 Å^2 as viewed along the *c* axis, respectively. Each iron(III) cation coordinates to four pyrroles of a porphyrin unit and one water molecule in a square-pyramidal geometry. As normally observed in the crystal structures of the heme cofactor in protein and iron-porphyrinic compounds,[20] the iron atom is out of the porphyrin plane with the mean deviation of 0.401 Å. *PLATON* calculations indicate that **3** contains 67.4% void space that is accessible to the solvent molecules.[19] TGA showed a weight loss of 18.6% occurred between 25 and 329 °C corresponding to the loss of DMF and H_2O molecules (expected 18.7%).

When cadmium nitrate was used instead of zinc nitrate under the identical reaction conditions to the synthesis of **3**, deep-brown crystals of compound **4** were formed after five days. Single-crystal X-ray diffraction analysis revealed that compound **4** crystallizes in the tetragonal $I4_1/acd$ space group (Figure 3). Different to the coordination mode in **3**, each Fe^{III}–HTCPP performs as a pentadentate ligand to bridge five cadmium atoms with three carboxylate groups, whereas the remaining carboxylate group is protonated (part a of Figure 3). Similar to that of in **3**, the iron atom, which square-pyramidally coordinates to four pyrroles in the equatorial positions and one oxygen atom in the axial site, is out of the porphyrin plane with the mean deviation of 0.5424 Å. Two Fe–HTCPP ligands are coupled by a μ_2-oxo to form a dimer, which is common in the iron-porphyrin based complexes.[21] The porphyrin pair connects with 10 Cd cations to form a lamellar network (part b of Figure 3). The porphyrin pairs are operated by the screw 4_1 axis to form an ...ABCDABCD... stacking pattern (part c of Figure 3). As a result, the lamellae are stacking into an interesting 3D framework structure comprising of micropores to accommodate guest molecules (part d of Figure 3). Calculations showed that the effective void space for the solvent molecules is 49.3% of the crystal volume. TGA chart indicates that a weight loss of 18.7% occurred between 30 and 329 °C corresponding to the release of DMF and water molecules (expected 18.9%).

We have tried to confirm the purity of the bulk crystalline samples **1**–**4** by comparing the simulated and experimental PXRD patterns. However, some diffraction peaks are not well matched between the simulated and experimental patterns even though we tried numerous times. To eliminate the impurity interference, we selected several very large crystals by hand under a microscope. The selected crystals were subjected to single-crystal X-ray diffraction study with consistent unit cell dimensions. The combined single crystals were used for PXRD experiments. However, there is no obvious improvement for the PXRD patterns ignoring the crystal size effect. Hence, we tentatively ascribed these phenomena to the inherent nature of these porphyrinic frameworks, such as the very strong background X-ray fluorescence of iron complexes.[22]

The access of different substrate molecules into the pores of the activated samples **1**–**4** was examined by sorption experiments. After the as-synthesized samples were activated at 90 °C under vacuum for 6 h, the solvent free samples were immersed in various solvents for 6 h at room temperature to study the guest inclusion property of **1**–**4**. GC-MS analysis indicates that the activated **1**–**4** can readily take up reasonable amount of different solvent molecules such as methanol, ethanol, acetonitrile, and benzene molecules as shown in Figure 4.

dx.doi.org/10.1021/ic3019502 | *Inorg. Chem.* 2013, 52, 3620–3626

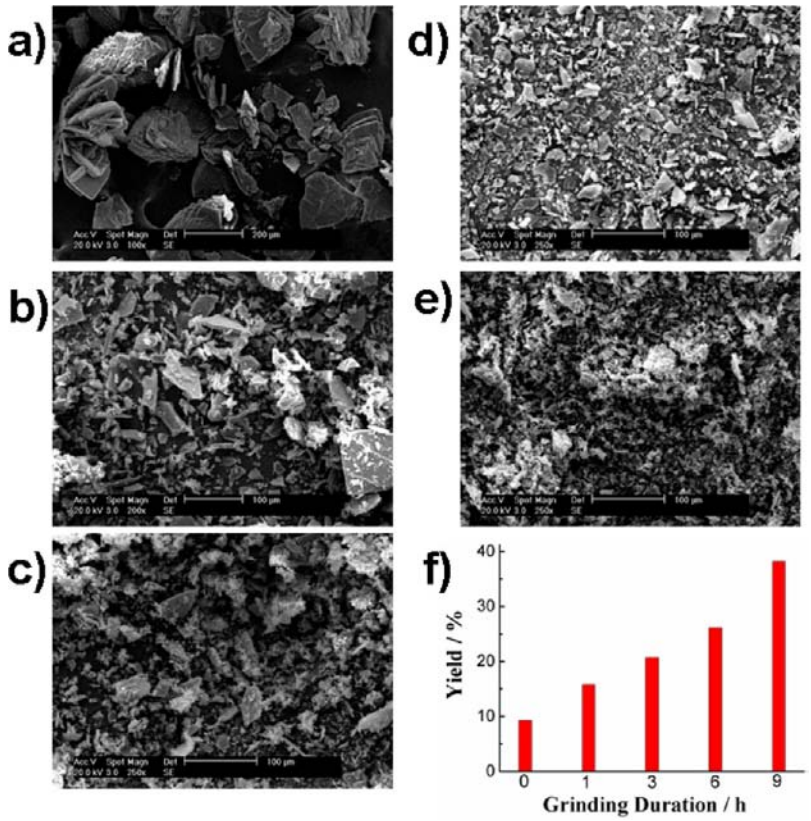

Figure 5. SEM images of **1** after magnetic stirring in CH_2Cl_2 at 200 rpm for 0 (a), 1 (b), 3 (c), 6 (d), and 9 (e) h, respectively; (f) Comparison of the catalytic activity of solid **1** with different particle sizes.

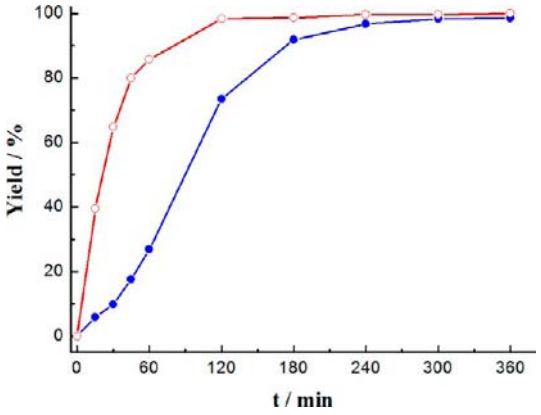

Figure 6. Traces of the styrene oxide yields versus reaction time catalyzed by freshly prepared (blue) and ground-up (red) samples of **1**.

It has been well established that homogeneous and heterogeneous metalloporphyrins are efficient catalysts for the selective oxidation of various hydrocarbons.[23] To test the catalytic ability of the four porphyrinic frameworks, they were used to oxidize styrene molecules with iodosobenzene (PhIO) oxidant. It is remarkable that styrene was fully oxidized into its epoxidized product by **1** and **2** in CH_2Cl_2 solvent at room temperature for 6 h (entries 1 and 2 in Table 1). However, compounds **3** and **4** are not efficient for the oxidation of styrene (entries 3 and 4 in Table 1). The less efficiency of iron-porphyrinic MOFs are similar to previous results.[24] We also observed that catalysts **3** and **4** are quickly deactivated by self-oxidation that is evident from bleaching out the reaction mixture. Under the same conditions, solid **1** can also oxidize a number of olefins with different sizes and dimensions (entries

Table 2. Aldol Reaction of Aldehydes and Ketones Catalyzed by Solids 1−4[a]

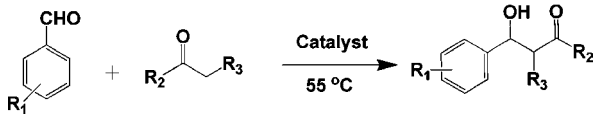

entry	R_1	R_2	R_3	catalyst	yield (d.r.)[b]
1	4-NO_2	Me	Me	**1**	55.0(43:57)
2	4-NO_2	Me	Me	**2**	55.0(43:57)
3	4-NO_2	Me	Me	**3**	99(73:27)
4	4-NO_2	Me	Me	**4**	82(52:48)
5	4-NO_2	Me	Me	FeCl−Me_4TCPP	5.3(83:17)
6	4-NO_2	Me	Me	MnCl−Me_4TCPP	13.7(57:43)
7	4-NO_2	Me	Me	$Zn(NO_3)_2{\cdot}6H_2O$	56.0(66:34)
8	4-NO_2	Me	Me	$Cd(NO_3)_2{\cdot}4H_2O$	4.8(60:40)
9	4-NO_2	Me	Me	$MnCl_2{\cdot}4H_2O$	5.4(69:31)
10	4-NO_2	Me	Me	$FeCl_3{\cdot}6H_2O$	N.D.[c]
11	3-NO_2	Me	Me	**3**	97(53:47)
12	2-NO_2	Me	Me	**3**	96(51:49)
13	2,4-NO_2	Me	Me	**3**	99(53:47)
14	4-NO_2	$-(C_2H_4)_4-$	**3**	96(61:39)	
15	4-NO_2	$-(C_2H_4)_3-$	**3**	91(52:48)	
16	4-NO_2	Me	Me	**3**	97(53:47)[d]

[a]Aldehyde (0.05 mmol) and catalyst (0.005 mmol) were stirred in ketone (1 mL) at 55 °C for 72 h. [b]Yields % and d.r. values were determined by HPLC using an Ultimate XB-C18 column (5 μm, 4.6 × 250 mm^2), average values of three runs. [c]Not determined. [d]The sixth cycle.

dx.doi.org/10.1021/ic3019502 | Inorg. Chem. 2013, 52, 3620−3626

3−12 in Table 1). More interestingly, solid **1** can oxidize the most inert cyclohexane molecules at room temperature with 20.6% substrate conversion (Scheme 1).

To understand the heterogeneous nature of the catalyst system, a mixture of solid **1** and PhIO in CH_2Cl_2 was stirred at room temperature for 12 h. After the solid was removed by filtration, styrene and additional PhIO were subsequently added into the filtrate, which was stirred for another 12 h at room temperature. GC analysis cannot detect a trace of product. After the solid catalyst was removed by filtration, the interrupted catalysis (after 45 min) cannot be preceded under the same conditions, even though additional oxidant was added. Above experiments thus demonstrate the heterogeneous catalytic nature of **1**. To make a comparison, MnCl−Me_4**TCPP** was employed as a homogeneous catalyst to oxidize these olefin molecules. The catalytic efficiency is much inferior to that of the heterogeneous catalysts in most cases (Table 1). These results unambiguously supported the heterogeneous behavior of these solid catalysts.

Catalyst **1** can be simply recovered by filtration, which was subsequently used in the successive run. However, the recovered solid lost its catalytic activity very quickly. The identical PXRD patterns of the recovered and freshly prepared samples of **1** suggest that the framework structure of the catalyst remained after the catalytic cycle (Figure S8 of the Supporting Information). Hence, the inactivation of the recovered catalyst should be ascribed to the active metal sites that are blocked by insoluble oxidant and/or insoluble product during oxidation process.[25]

Although the manganese(III) sites are well-dispersed in the porous frameworks, the axial coordination sites are ligated by the formate pillars in the 3D nets of **1** and **2**. Hence, the Mn^{III} sites in the channel walls are inaccessible to the substrate molecules, even though their vacant spaces can accommodate enough amount of solvent molecules.[18] Hence, the catalysis should occur on the exterior solid surfaces of **1** and **2**. To further understand the exterior solid surface prompted process, we studied the relationship between particle size and catalytic efficiency.[25b] The particle sizes of solid **1** were controlled by grinding duration in CH_2Cl_2 at room temperature and monitored by SEM images (Figure 5). To avoid exposing new surface catalytic sites, the catalytic reaction was performed without stirring under the otherwise identical conditions. GC analysis of the supernatants showed that the product yield increases upon decreasing the particle sizes. We also compared the catalytic efficiency of the as-synthesized and pretreated samples. The different reaction rates further demonstrate the particle-size-effect of the catalysis platform (Figure 6).

Because compounds **3** and **4** are not stable under above oxidation conditions, we have therefore tried the intermolecular aldol reaction of aldehydes and ketones to evaluate their catalytic property.[26] The reaction of *p*-nitrobenzaldehyde and 2-butanone with solid catalyst **3** proceeds smoothly at 55 °C under solvent free conditions. As shown in Table 2, the catalytic activity of **3** is the best among the four solid catalysts (entries 1−4). The yield of aldol product is excellent (99%) with outstanding product regioselectivity of 100% for **3**. The catalytic efficiency of **3** is also much superior to the constituents of these porphyrinic MOFs, such as FeCl−Me_4TCPP, MnCl−Me_4TCPP, $Zn(NO_3)_2{\cdot}6H_2O$, $Cd(NO_3)_2{\cdot}4H_2O$, and $MnCl_2{\cdot}4H_2O$ (entries 5−9 in Table 2). We also used $FeCl_3{\cdot}6H_2O$ as catalyst under the reaction conditions (entry 10 in Table 2). However, the catalytic products are a very complicated mixture that cannot be simply separated and characterized. Above results suggest that high catalytic activity of **3** should be attributed to the synergistic effect of the multiple Lewis acid centers. Because the M′ cations within the pores are inaccessible to substrate molecules, the catalysis occurs on the exterior solid surfaces.

Compound **3** can also catalyze the aldol reaction between various nitrobenzaldehydes and ketones with excellent substrate conversions (entries 11−15 in Table 2). Catalyst **3** can be easily recovered by filtration, which was subsequently used in the successive runs. The recovered catalyst did not decrease the catalytic activity in the following six runs (entry 16 in Table 2). To test its heterogeneous nature, compound **3** was stirred in 2-butanone at 55 °C for 72 h, and the mixture was filtered. *p*-Nitrobenzaldehyde was added into the hot filtrate, which was heated at 55 °C for another 72 h under stirring. HPLC analysis cannot detect a trace of product, which proved that the present catalyst platform is heterogeneous in nature.

CONCLUSIONS

In summary, we synthesized four metalloporphyrin functionalized MOFs with interesting catalytic property. Compounds **1**−**3** are built up from $M'_2(COO)_4$ paddle-wheel SBUs bridged by M−TCPP ligands and formate pillars. According to their binding affinity, the formate pillar heterogeneously bridges Mn and M′ (M′ = Zn and Cd) cations in **1** and **2**, whereas the formate pillar homogeneously bridges M′ cations in **3**. Despite the fact that compounds **1** and **2** are highly porous; however, the substrate molecules cannot access the inner Mn^{III} metal sites because they are ligated by formate pillars. Hence, the epoxidation of olefins occurs on the exterior solid surfaces with excellent conversion and selectivity. Although the porphyrin Fe^{III} cations are readily available for substrate molecules, the catalysts are not stable under the epoxidation conditions. We therefore probed the catalytic property by the intermolecular aldol reaction of aldehydes and ketones with excellent substrate conversions for **3**. This work complements the current shortcoming on the issue of the catalysis in the inner pores or on the exterior solid surfaces of MOF catalysts.

ASSOCIATED CONTENT

Supporting Information

Additional figures, table, and crystallographic data in CIF format. This material is available free of charge via the Internet at http://pubs.acs.org.

AUTHOR INFORMATION

Corresponding Author

*E-mail: maan@petrochina.com.cn (M.A.), cdwu@zju.edu.cn (C.-D.W.).

Notes

The authors declare no competing financial interest.

ACKNOWLEDGMENTS

We are grateful for the financial support of the NSF of China (Grant No. 21073158), Zhejiang Provincial Natural Science Foundation of China (Grant No. Z4100038), and the Specialized Research Fund for the Doctoral Program of Higher Education of China (Grant No. 20090101110017).

REFERENCES

(1) (a) O'Keeffe, M.; Yaghi, O. M. *Chem. Rev.* **2012**, *112*, 675. (b) Stock, N.; Biswas, S. *Chem. Rev.* **2012**, *112*, 933. (c) Perry, J. J., IV; Perman, J. A.; Zaworotko, M. J. *Chem. Soc. Rev.* **2009**, *38*, 1400.

(2) (a) Yoon, M.; Srirambalaji, R.; Kim, K. *Chem. Rev.* **2012**, *112*, 1196. (b) Uemura, T.; Yanai, N.; Kitagawa, S. *Chem. Soc. Rev.* **2009**, *38*, 1228. (c) Ma, L.; Abney, C.; Lin, W. *Chem. Soc. Rev.* **2009**, *38*, 1248. (d) Lee, J.; Farha, O. K.; Roberts, J.; Scheidt, K. A.; Nguyen, S. T.; Hupp, J. T. *Chem. Soc. Rev.* **2009**, *38*, 1450. (e) Wang, Z.; Chen, G.; Ding, K. *Chem. Rev.* **2009**, *109*, 322. (f) Corma, A.; García, H.; Llabrés i Xamena, F. X. *Chem. Rev.* **2010**, *110*, 4606.

(3) (a) Allendorf, M. D.; Bauer, C. A.; Bhakta, R. K.; Houk, R. J. T. *Chem. Soc. Rev.* **2009**, *38*, 1330. (b) Cui, Y.; Yue, Y.; Qian, G.; Chen, B. *Chem. Rev.* **2012**, *112*, 1126.

(4) (a) Murray, L. J.; Dincă, M.; Long, J. R. *Chem. Soc. Rev.* **2009**, *38*, 1294. (b) Li, J.-R.; Kuppler, R. J.; Zhou, H.-C. *Chem. Soc. Rev.* **2009**, *38*, 1477. (c) Sumida, K.; Rogow, D. L.; Mason, J. A.; McDonald, T. M.; Bolch, E. D.; Herm, Z. R.; Bae, T.-H.; Long, J. R. *Chem. Rev.* **2012**, *112*, 724. (d) Suh, M. P.; Park, H. J.; Prasad, T. K.; Lim, D.-W. *Chem. Rev.* **2012**, *112*, 782.

(5) (a) Chen, B.; Xiang, S.; Qian, G. *Acc. Chem. Res.* **2010**, *43*, 1115. (b) Kreno, L. E.; Leong, K.; Farha, O. K.; Allendorf, M.; Van Duyne, R. P.; Hupp, J. T. *Chem. Rev.* **2012**, *112*, 1105.

(6) (a) Kurmoo, M. *Chem. Soc. Rev.* **2009**, *38*, 1353. (b) *Metal–Organic and Organic Molecular Magnets*; Day, P., Underhill, A. E., Ed.; Royal Society of Chemistry: Cambridge, UK, 2000; vol. *252*. (c) Zhang, W.; Xiong, R.-G. *Chem. Rev.* **2012**, *112*, 1163.

(7) (a) Wu, C.-D.; Hu, A.; Zhang, L.; Lin, W. *J. Am. Chem. Soc.* **2005**, *127*, 8940. (b) Song, F.; Wang, C.; Falkowski, J. M.; Ma, L.; Lin, W. *J. Am. Chem. Soc.* **2010**, *132*, 15390. (c) Shi, L.-X.; Wu, C.-D. *Chem. Commun.* **2011**, *47*, 2928.

(8) (a) Wu, C.-D.; Li, L.; Shi, L.-X. *Dalton Trans.* **2009**, 6790. (b) Wang, M.; Xie, M.-H.; Wu, C.-D.; Wang, Y.-G. *Chem. Commun.* **2009**, 2396.

(9) (a) Sessler, J. L.; Seidel, D. *Angew. Chem., Int. Ed.* **2003**, *42*, 5134. (b) Lemon, C. M.; Brothers, P. J.; Boitrel, B. *Dalton Trans.* **2011**, *40*, 6591. (c) Lee, C. H. *Bull. Korean Chem. Soc.* **2011**, *32*, 768. (d) Sessler, J. L.; Camiolo, S.; Gale, P. A. *Coord. Chem. Rev.* **2003**, *240*, 17. (e) Sessler, J. L.; Miller, R. A. *Biochem. Pharmacol.* **2000**, *59*, 733. (f) Han, H.; Hurley, L. H. *Trends Pharmacol. Sci.* **2000**, *21*, 136. (g) Lane, B. S.; Burgess, K. *Chem. Rev.* **2003**, *103*, 2457. (h) Eichhorn, H. *J. Porphyrins Phthalocyanines* **2000**, *4*, 88. (i) Sandanayaka, A. S. D.; Ito, O. *J. Porphyrins Phthalocyanines* **2009**, *13*, 1017. (j) Yan, G.-P.; Li, Z.; Xu, W.; Zhou, C.-K.; Yang, L.; Zhang, Q.; Li, L.; Liu, F.; Han, L.; Ge, Y.-X.; Guo, J.-F. *Int. J. Pharm.* **2011**, *407*, 119. (k) Lo, P.-C.; Leng, X.; Ng, D. K. P. *Coord. Chem. Rev.* **2007**, *251*, 2334. (l) Wagenknecht, H.-A. *Angew. Chem., Int. Ed.* **2009**, *48*, 2838. (m) Sun, R. W.-Y.; Che, C.-M. *Coord. Chem. Rev.* **2009**, *253*, 1682. (n) Zou, C.; Wu, C.-D. *Dalton Trans.* **2012**, *41*, 3879.

(10) (a) Shultz, A. M.; Farha, O. K.; Hupp, J. T.; Nguyen, S. T. *J. Am. Chem. Soc.* **2009**, *131*, 4204. (b) Alkordi, M. H.; Liu, Y.; Larsen, R. W.; Eubank, J. F.; Eddaoudi, M. *J. Am. Chem. Soc.* **2008**, *130*, 12639. (c) Larsen, R. W.; Wojtas, L.; Perman, J.; Musselman, R. L.; Zaworotko, M. J.; Vetromile, C. M. *J. Am. Chem. Soc.* **2011**, *133*, 10356. (d) Larsen, R. W.; Wojtas, L.; Perman, J.; Musselman, R. L.; Zaworotko, M. J.; Vetromile, C. M. *J. Am. Chem. Soc.* **2011**, *133*, 10356. (e) Zhang, Z.; Zhang, L.; Wojtas, L.; Nugent, P.; Eddaoudi, M.; Zaworotko, M. J. *J. Am. Chem. Soc.* **2012**, *134*, 924. (f) Zhang, Z.; Zhang, L.; Wojtas, L.; Eddaoudi, M.; Zaworotko, M. J. *J. Am. Chem. Soc.* **2012**, *134*, 928. (g) Symthe, N. C.; Butler, D. P.; Moore, C. E.; McGowan, W. R.; Rheingold, A. L.; Beauvais, L. G. *Dalton Trans.* **2012**, *41*, 7855.

(11) (a) Xie, M.-H.; Yang, X.-L.; Zou, C.; Wu, C.-D. *Inorg. Chem.* **2011**, *50*, 5318. (b) Zou, C.; Zhang, Z.; Xu, X.; Gong, Q.; Li, J.; Wu, C.-D. *J. Am. Chem. Soc.* **2012**, *134*, 87. (c) Xie, M.-H.; Yang, X.-L.; Wu, C.-D. *Chem. Commun.* **2011**, *47*, 5521. (d) Yang, X.-L.; Xie, M.-H.; Zou, C.; He, Y.; Chen, B.; O'Keeffe, M.; Wu, C.-D. *J. Am. Chem. Soc.* **2012**, *134*, 10638. (e) Zou, C.; Xie, M.-H.; Kong, G.-Q.; Wu, C.-D. *CrystEngComm* **2012**, *14*, 4850–4856.

(12) (a) Gauuan, P. J. F.; Trova, M. P.; Gregor-Boros, L.; Bocckino, S. B.; Crapo, J. D.; Day, B. J. *Bioorg. Med. Chem.* **2002**, *10*, 3013. (b) Kumar, A.; Maji, S.; Dubey, P.; Abhilah, G. J.; Pandey, S.; Sarkar, S. *Tetrahedron Lett.* **2007**, *48*, 7287.

(13) *CrysAlisPro*, version 1.171.34.44; Oxford Diffraction Ltd.: Oxfordshire, U.K., 2010.

(14) Sheldrick, G. M. *Program for Structure Refinement*; University of Göttingen: Germany, 1997.

(15) Spek, A. L. *J. Appl. Crystallogr.* **2003**, *36*, 7.

(16) Crystal data for **1**: $C_{67}H_{73}MnN_{10}O_{19}Zn_2$, M = 1508.03, tetragonal, space group $I4/mmm$, a = 16.6701(12) Å, c = 15.481(2) Å, V = 4302.0(7) Å^3, Z = 2, μ = 0.761 mm^{-1}. The final R_1 = 0.0358, $wR2$ = 0.0870, and S = 1.041 for 759 observed reflections. Crystal data for **2**: $C_{67}H_{75}Cd_2MnN_{10}O_{20}$, M = 1620.11, tetragonal, space group $I4/mmm$, a = 16.9198(4) Å, c = 16.0170(6) Å, V = 4585.3(2) Å^3, Z = 2, μ = 0.656 mm^{-1}. The final R_1 = 0.0392, $wR2$ = 0.1176, and S = 1.180 for 1139 observed reflections. Crystal data for **3**: $C_{58}H_{50}FeN_7O_{15}Zn_2$, M = 1271.64, tetragonal, space group $P4/mmm$, a = 16.6651(5) Å, c = 8.8573(11) Å, V = 2459.9(3) Å^3, and Z = 1, μ = 2.098 mm^{-1}. The final R_1 = 0.1285, $wR2$ = 0.2387, and S = 1.003 with 65 parameters for 1002 observed reflections. Crystal data for **4**: $C_{111}H_{97}Cd_3Fe_2N_{13}O_{28}$, M = 2509.92, tetragonal, space group $I4_1/acd$, a = 41.445(1) Å, c = 32.834(3) Å, V = 56400(6) Å^3, and Z = 16, μ = 0.710 mm^{-1}. The final R_1 = 0.1418, $wR2$ = 0.2426, and S = 1.038 with 220 parameters for 1887 observed reflections.

(17) The anionic formate should be a thermal decomposition product of DMF. When zinc nitrate in DMF was heated at 80 °C for one week, a 3D anionic framework of zinc formate was formed in very high yield. Crystal data: $C_5H_{11}NO_6Zn$, M_r = 246.52, hexagonal, space group R-3c, a = 8.1913(3) Å, c = 22.266(1) Å, V = 1293.83(9) Å^3, and Z = 6, R_1 = 0.0255, $wR2$ = 0.0709, and S = 1.098. See also: Jain, P.; Dalal, N. S.; Toby, B. H.; Kroto, H. W.; Cheetham, A. K. *J. Am. Chem. Soc.* **2008**, *130*, 10450.

(18) (a) Barron, P. M.; Son, H.-T.; Hu, C.; Choe, W. *Cryst. Growth Des.* **2009**, *9*, 1960. (b) Choi, E.-Y.; Barron, P. M.; Novotny, R. W.; Son, H.-T.; Hu, C.; Choe, W. *Inorg. Chem.* **2009**, *48*, 426.

(19) Spek, A. L. *PLATON, A Multipurpose Crystallographic Tool*; Utrecht University: Utrecht, The Netherlands, 2008.

(20) (a) Cupp-Vickery, J. R.; Poulos, T. L. *Nat. Struct. Biol.* **1995**, *2*, 144. (b) Evans, D. R.; Reed, C. A. *J. Am. Chem. Soc.* **2000**, *122*, 4660. (c) Hu, C.; Noll, B. C.; Schulz, C. E.; Scheidt, W. R. *Inorg. Chem.* **2010**, *49*, 10984. (d) Walker, V. E. J.; Castillo, N.; Matta, C. F.; Boyd, R. J. *J. Phys. Chem. A* **2010**, *114*, 10315.

(21) (a) Deng, Y.; Chang, C. J.; Nocera, D. G. *J. Am. Chem. Soc.* **2000**, *122*, 410. (b) Ghosh, S. K.; Patra, R.; Rath, S. P. *Inorg. Chem.* **2008**, *47*, 10196.

(22) Klug, H. P, Alexander, L. E. *X-Ray Diffraction Procedures: For Polycrystalline and Amorphous Materials*, 2nd ed.; John Wiley and Sons: New York, 1974.

(23) (a) Che, C.-M.; Huang, J.-S. *Chem. Commun.* **2009**, 3996. (b) Xia, Q.-H.; Ge, H.-Q.; Ye, C.-P.; Liu, Z.-M.; Su, K.-X. *Chem. Rev.* **2005**, *105*, 1603. (c) Rose, E.; Andrioletti, B.; Zrig, S.; Quelquejeu-Ethève, M. *Chem. Soc. Rev.* **2005**, *34*, 573. (d) Costas, M. *Coord. Chem. Rev.* **2011**, *255*, 2912.

(24) Farha, O. K.; Shultz, A. M.; Sarjeant, A. A.; Nguyen, S. T.; Hupp, J. T. *J. Am. Chem. Soc.* **2011**, *133*, 5652.

(25) (a) Wang, C.; Xie, Z.; deKrafft, K. E.; Lin, W. *J. Am. Chem. Soc.* **2011**, *133*, 13445. (b) Suslick, K. S.; Bhyrappa, P.; Chou, J.-H.; Kosal, M. E.; Nakagaki, S.; Smithenry, D. W.; Wilson, S. R. *Acc. Chem. Res.* **2005**, *38*, 283.

(26) (a) *Lewis Acids in Organic Synthesis*; Yamamoto, H., Ed.; Wiley: Weinheim, 2000. (b) *Encyclopedia of Reagents for Organic Synthesis*; Paquette, L. A., Ed.; John Wiley & Sons: Chichester, 1995. (c) Notz, W.; Tanaka, F.; Barbas, C. F. *Acc. Chem. Res.* **2004**, *37*, 580.